Acoustic and velocity field over 3D cavities

Rajarshi Das,[a)] and Job Kurian[b)]
Department of Aerospace Engineering, Indian Institute of Technology, Madras, Chennai 600036, India

(Received 5 April 2012; accepted 4 December 2012; published online 10 January 2013)

Abstract Effects of wall mounted cavity on a Mach 1.7 freestream flow over it are investigated experimentally and numerically. Three different three dimensional (3D) cavity configurations have been used in the study. The results are compared with those of a two dimensional (2D) cavity. Flow field over the cavity is observed to depend intensely on the cavity width and on the allied aerodynamic flow structure in the vicinity of the cavity. Pressure oscillations generated by presence of wall mounted cavity in supersonic freestream was also observed to affect the fluid motion over cavities. [doi:10.1063/2.1301201]

Keywords cavity, supersonic flow, pressure oscillations, fluid motion

Acoustic excitation of supersonic flow in the vicinity of wall mounted cavities and its possible causes have been investigated extensively in recent years due to its potential use as fuel air mixing and flameholding tool in scramjet engines. Excitation of the flow creates unsteadiness, induces turbulence and exchange of fluid between cavity and the mainstream. Pressure oscillations generated due to presence of cavities in the flow path have been established as the root cause of this flow excitation.[1] Generation of these acoustic oscillations is due to the interaction of the free shear layer with the cavity trailing edge[2] and the periodic inflow and outflow of fluid into and out of the cavity due to fluctuating motion of the shear layer.[3] Fluid mass entering the cavity from the mainstream in association with large scale vortex formation at the cavity leading edge and its subsequent shedding and ejection from the cavity near the trailing edge were observed by Rowley et al.[4] Sato et al.[5] experimentally demonstrated the acoustic excitation of flow in terms of enhancement in the shear layer growth rate when the oscillations generated by a flow past cavity are directed at the initial mixing layer between the two co-flowing supersonic streams. Most of the earlier work in this area has been confined to 2D cavities.

Of the very few studies done on flow over 3D cavities, Block[6] observed that the frequencies of oscillation are independent of cavity width for subsonic freestream flow. Change in frequency of dominant mode of oscillation with change in cavity width was observed by Woo et al.[7] in the case of flow over cavities at supersonic Mach number of 1.5. In a similar study on wall mounted 3D cavities placed in a supersonic flow field, multiple modes of oscillations were observed for a free stream Mach number of 1.2.[8]

The present study is aimed at a good understanding of supersonic flow over wall mounted cavities with regard to the acoustic field generated in the vicinity. The fluid flow induced by the cavity oscillations is also studied numerically and experimentally. The influence of the width of the cavity on these fluid dynamic features is expected to provide an effective input to the designers of mixing and flame holding devices.

Schematic of the test section along the axial plane is shown in Fig. 1. The Mach 1.7 flow is maintained in the test section of cross section 60 mm × 30 mm at a flow Reynolds number of $1.180\,5 \times 10^6$. Cavities of length 50 mm and depth 25 mm were used for the study. The width of the cavities was kept at 25 mm, 16.7 mm and 12.5 mm in different sets of experiments thereby giving L/W ratios of 2, 3 and 4 for the three 3D cases. For the 2D configuration, the cavity spanned the entire width of the test section thus giving and L/W ratio of less than 1. The L/D ratio of the cavity was kept constant at 2 for all the test cases. A 3D isometric view of the test section is shown in Fig. 2 where x, y and z denotes the lateral, transverse and the axial directions, respectively.

Velocity components in a plane 2 mm above the cavity in the freestream measured using trust science innovation (TSI) make laser doppler velocimeter (LDV). The LDV system utilizes the 488 and 514.5 nm beams of a 5 W Innova 70 C series argon ion laser in the back scattering mode. A 40 MHz shift is added to one beam of each colour to remove directional ambiguity. A 50 mm beam spacing and 363 mm focal length result in a measurement volume diameter of 9.53×10^{-2} mm. Separate TSI make seeder unit is used to inject oil droplets of about 1micron size into the flow which served as the tracer particle for velocity measurement. Velocity components measured were along the axial z and lateral x directions parallel to the test section floor. The measurement points are at locations 5 mm apart in each direction in a 65 mm × 60 mm plane above the cavity. Experimental uncertainty was found to vary within ±1% of measured velocity.

Unsteady pressure measurements were done using piezoelectric type transducers of PCB (piezotronics make, model 112A22) at the measurement ports on the leading and trailing edge walls as shown in Fig. 1. Two transducers were used to make measurements at two ports simultaneously. An NI-6024E A/D converter card was used to acquire the signals from the transducers. The maximum sampling frequency of the card was

a)Corresponding author. Email: drajarshi@sify.com.
b)Email: kurian@ae.iitm.ac.in.

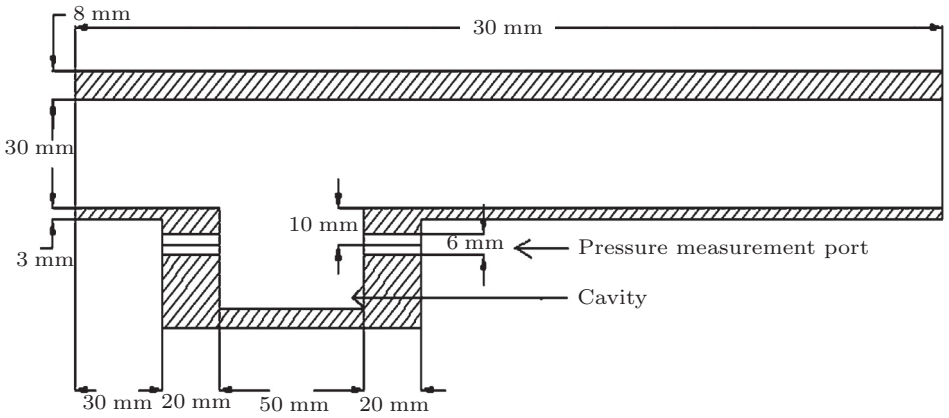

Fig. 1. Schematic of test section.

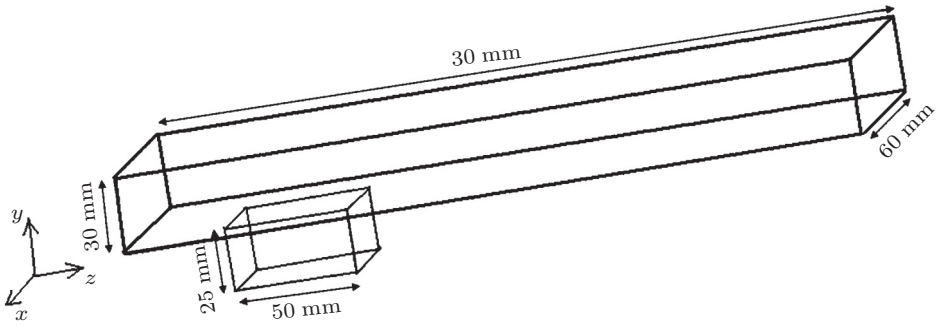

Fig. 2. Schematic diagram of three-dimensional cavity configuration.

200 kHz and a sampling rate of 100 kHz was available for each of the transducers. Signals were acquired for 0.5 s, thereby giving 5×10^4 samples for each run. The acquired signals were processed through a Matlab program where FFT algorithm was employed to identify the dominant frequencies and their amplitudes. Each data record was windowed into 48 segments of 1 024 samples each with a transform length of 2 048 samples. A Hamming window with 50% overlap is used for estimation of the spectra giving a frequency resolution of 48.82 Hz. Multiple runs were conducted under identical experimental conditions, under which variation in the frequencies of the dominant modes were observed to be within 10 Hz in the 0 to 50 kHz range. Experimental uncertainty in measuring amplitudes of the dominant modes was found to be within ±3%.

Spread of fluid over the cavity into the mainstream in the lateral x direction was investigated by measuring the lateral component of velocities in a plane 2 mm above the top edge of the cavity in the mainstream flow. The axial component was also measured to find the variation of fluid velocity in this direction. These velocities are time averaged; spread over 10^4 samples in a time period of 6 s for most of the cases. The axial velocity was observed to be (330±1) m/s for all the points where velocity was measured except immediately after the leading and trailing edges. Lateral velocity vectors are plotted and shown in Fig. 3. Axial velocity component was not superimposed on the lateral component as it was observed to be much higher than the lateral component. The vector length scale used for all the cases is 0.15 cm per unit magnitude of velocity (1 m/s).

Lateral flow is observed to be spread over the measurement plane as observed from Fig. 3. Fluid motion away from the cavity in the lateral direction is observed to be higher after a certain distance from the leading edge for the three cases. Flow visualization experiments performed as part of an earlier study showed an oblique shock at the leading edge of the cavity. The shock is caused due to the obstruction of the supersonic primary free stream by the oscillating shear layer.[9] High pressure region immediately after this shock could be the possible reason causing the flow after the shock to spill over to the adjoining region towards the test section sidewalls. At the trailing edge of the cavity, lateral flow is seen relatively higher for the widest cavity.

Lateral velocity vectors plotted in Fig. 3 shows that both magnitude and spatial spread of fluid are higher for the widest than the other two cavities. Quantitatively, the magnitude of lateral velocity was observed to be 19 m/s at a location 16 mm from the cavity leading edge for the $L/W = 2$ model. For the narrower models, though the lateral velocity was found to be maximum near the same location, the magnitude was much lower at 9 m/s. The shear layer deflection at the leading edge and the higher shock angle generated give rise to greater

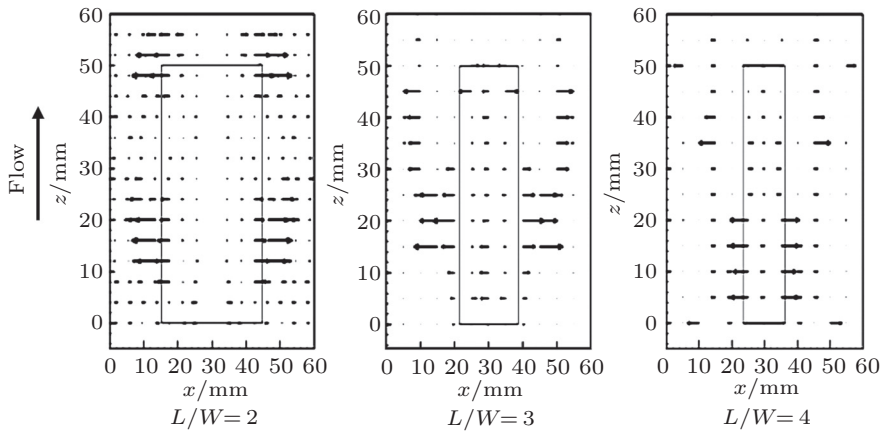

Fig. 3. Velocity vectors along a plane 2 mm above the cavity open top.

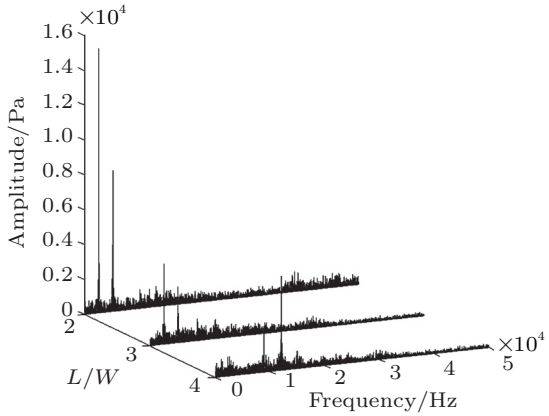

Fig. 4. Amplitude spectra of pressure oscillations (trailing edge).

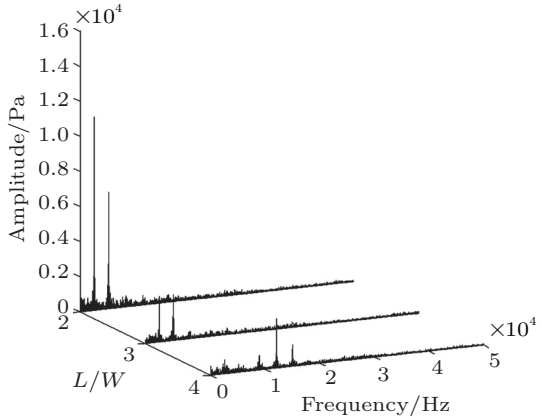

Fig. 5. Amplitude spectra of pressure oscillations (leading edge).

pressure gradient between the region aft of the leading edge shock and the region over the sidewalls for the $L/W = 2$ model.[9] Higher magnitude of lateral velocity for the $L/W = 2$ model is thus the effect of this high pressure gradient.

The amplitude spectrum of pressure signal obtained at the trailing edge port of all the 3D cavities is shown in Fig. 4. Occurrence of discrete magnitude peaks along with broadband fluctuations is observed in all the amplitude spectra. Existence of peaks and their periodicity emphasize a periodic wave structure in all the cavities. Generation of these waves is due to the dynamic nature of the shear layer and its interaction with the trailing edge.

From Fig. 4 it is evident that as the cavity became narrower, the pressure oscillation moved to a higher dominant mode with a change in frequency. A sharp decline in amplitude of the dominant mode is also observed as the cavity L/W ratio changes from 2 to 3. Amplitude spectrum for the leading edge pressure port is shown in Fig. 5. It is observed that the dominant modes are same as the trailing edge with only a decrease in amplitude of all the modes. The frequency of different modes of oscillations at leading and trailing edge is observed to be identical for each of the three models. Modes 3, 4 and 5 are barely visible in Fig. 4 due to very high amplitude of the dominant mode of oscillation for the L/W 2 model.

A comparative study of the values of the amplitudes and frequency of different modes of oscillations at the trailing edge for all the three cavities is shown in Table 1. It is observed that the sound pressure level (SPL), $SPL = 20 \lg (P_{\rm rms}/20\ \mu{\rm Pa})$ of the dominant mode for the widest cavity is 177.6 dB as compared to 169.2 dB and 168.6 dB for the other two cavities.

Similarly for the 2D cavity, the first mode of oscillation is found to be dominant as shown in Fig. 6. In comparison with the widest 3D cavity of L/W ratio 2, the magnitude of the dominant mode for the 2D cavity was observed to be much lower at 168.5 dB at a frequency of 2 542 Hz.

Flow field in the test section is numerically simulated using commercially available finite volume code FLUENT. Unsteady Reynolds averaged Navier–Stokes (RANS) is used as the preferred numerical technique due to unsteady nature of the flow marked by periodic

Table 1. Frequency and SPL of oscillations at different modes.

Modes	$L/W = 2$		$L/W = 3$		$L/W = 4$	
	Frequency/Hz	SPL/dB	Frequency/Hz	SPL/dB	Frequency/Hz	SPL/dB
1	2 542	177.6	2 542	169.2	2 542	154.9
2	5 181	172.1	5 181	164.1	—	—
3	—	—	8 602	155.9	8 895	161.0
4	—	—	11 930	154.9	12 020	168.6
5	—	—	14 860	151.6	14 900	154.1

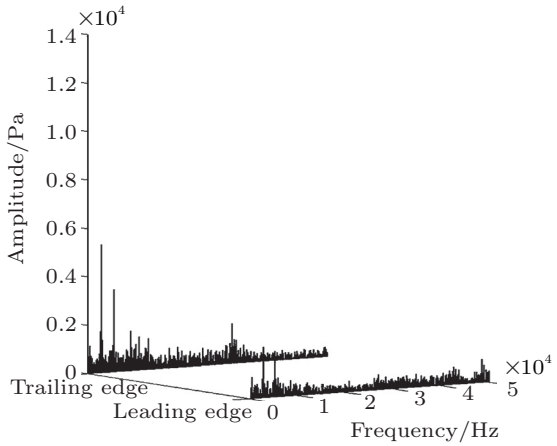

Fig. 6. Amplitude spectra of pressure oscillation for 2D cavity.

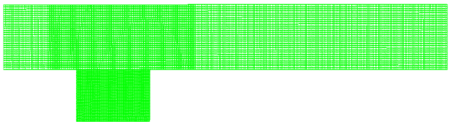

Fig. 7. Computational grid along the axial plane of the test section.

vortex shedding and self sustaining pressure oscillations. Explicit scheme has been used for time marching and the results obtained has been displayed as time averaged flow structure after the flow parameters converged to the desired boundary conditions. Geometrical configurations of all the models are generated using Gambit, commercially available modeling software. The computational domain is meshed into structured hexahedral cells using GAMBIT. The number of cells varied from 687 600 for the narrowest cavity to 918 000 for the widest cavity (2D configuration) after grid independence and grid adaptation studies were done. Computational grid for the widest 3D cavity is shown in Fig. 7. Fine grid was used in the vicinity of the cavity to capture flow structure accurately.

Standard k–ε model is used to determine turbulence in the test section flow at $Ma = 1.7$ with a stagnation pressure of 5.0 bar (gauge). Pressure inlet and pressure outlet were used as boundary conditions at entry and exit. The working fluid is air under ideal gas conditions. In the present simulation, convergence is considered when the difference in mass flow rate at inlet and outlet is less than 0.1% of the inlet mass flow rate and the residual values falls to 10^{-6}. Grid adaptation study is done till the wall y^+ values 10 mm upstream of the cavity leading edge for all the models came down to below 19.

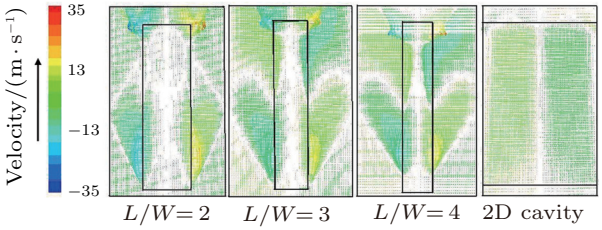

Fig. 8. Lateral velocity vectors in a plane 2 mm above the test section floor.

Spillage of fluid over the cavity sidewalls and the reason behind such fluid movement is looked into from the results obtained during numerical simulation. The lateral velocity vectors obtained along the horizontal plane 2 mm above the cavity for all the test sections are shown in Fig. 8. The primary freestream flow above the cavity is from the bottom to the top of the page as marked by an arrow on the left of the colour bar in Fig. 8. The colour bar denotes the velocity range in m/s. The cavity top surface for each of the test cases is also shown in the figure. Fluid motion in the lateral direction away from the cavity towards the test section walls for the 3D cavities is evident from the velocity vectors shown in Fig. 8. Lateral movement of fluid for the 2D cavity configuration is almost insignificant thereby establishing a predominantly 2D flow structure over the cavity.

For the 3D cavity configurations, the fluid coming out of the cavity is observed to spill over the cavity sidewalls immediately after the leading edge but the location of initiation of this spillage moves aft of the leading edge as the cavity narrows down. The decrease in shock angle with the narrowing down of the cavity as discussed implies that the high pressure region above will be lit-

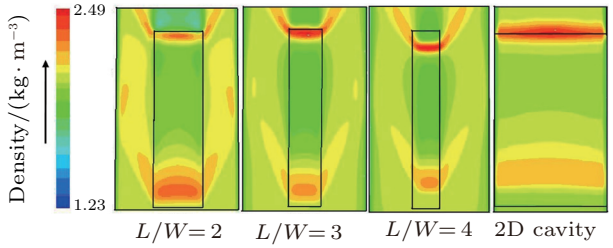

Fig. 9. Filled contours of density along a plane 2 mm above the test section floor.

tle downstream as compared to the wider 3D cavities. This was further investigated by plotting the density contours along the same plane as shown in Fig. 9.

The colour bar in Fig. 9 gives the range of density in kg/m^3. The variation in density also shows a shift in the location of high density region aft of the cavity leading edge due to a lower shock angle for the narrower cavities. Density contours for the 2D configuration also show the high density region little aft of the leading edge. As one moves downstream along the length of the 3D cavities, a reversal in direction of fluid motion is observed beyond a point half the cavity length for the $L/W = 3$ and $L/W = 4$ models. This may be due to the downward movement of the shear layer into the cavity in this region which is also manifested by the severe density gradient at the trailing edge for these two models. As the shear layer dives into the cavity near the trailing edge, a bow shock is generated due to obstruction to the supersonic incoming stream by the trailing edge. This bow shock generates a high density gradient upstream of the trailing edge which is observed in Fig. 9 for the narrow cavity configurations. Fluid motion away from the cavity towards the test section walls is observed immediately aft of this high density gradient region.

The supersonic flow field over 3D cavities has been investigated both experimentally and numerically. Spillage of flow over the sidewalls of the cavities downstream of the cavity leading edge is observed. The quantum of fluid flow is believed to be dependent on the nature of shock generated due to the presence of cavity. High amplitude of pressure oscillations generated within the 3D cavity may thus be the source controlling the shear layer behavior, the shock formation and thus the spillage of flow over the cavity walls. The acoustics generated and the fluid velocities induced have strong dependence on the width of the 3D cavities.

1. E. Gutmark, K. C. Schadow, and K. H. Yu, Annual Review of Fluid Mechanics **27**, 375 (1995).
2. J. E. Rossiter, Wind tunnel experiments on the flow over rectangular cavities at subsonic and transonic speeds, RAE Tech. Report 64037 (1964).
3. A. J. Bilanin, and E. E. Covert, AIAA Journal **11**, 3 (1973).
4. C. W. Rowley, T. Colonius, and A. J. Basu, Journal of Fluid Mechanics **455**, 315 (2002).
5. N. Sato, R. Imamura, and S. Shiba, et al., AIAA-96-4510 (1996).
6. P. J. W. Block, Noise response of cavities of varying dimensions at subsonic speeds, NASA TN D 8351 (1976).
7. C. Woo, J. Kim, and K. Lee, Journal of Mech. Science and Tech. **22**, 590 (2008).
8. B. I. Soemarwoto, and J. C. Kok, Computations of three- dimensional unsteady supersonic cavity flow to study the effect of downstream geometries, NLR-TP-2001-446 (2001).
9. R. Das, and J. Kurian, in: *Proc. of 20th International Symposium of Air Breathing Engines*, Paper No.1517 (2011).